Bioengineering Research

An Isotropic Hyperelastic Model of Esophagus Tissue Layers along with three-dimensional Simulation of Esophageal Peristaltic Behavior

Peiman HajHosseini [1], **Meisam Takalloozadeh** [2,*]

[1]Research Engineer; Young Researchers and Elite Club Central Tehran Branch, Islamic Azad University, Tehran, Iran
[2]Assistant Professor at Shiraz University

Correspondence to: HajHosseini P. (E-mail: peiman.hh@gmail.com)

Abstract

Understanding mechanical characterization of the esophagus tissue layers is a step forward to the development of esophageal behavior, peristaltic simulation, and advanced clinical practices. Esophagus tissue layers behave nonlinear with a large amount of malformation. In this paper, different models based on the hyperelastic theory are discussed and compared to investigate the accuracy of the simulations in esophagus tissue mechanics. The simulated tissues were assumed as nonlinear, incompressible, and homogenous isotropic material. We have used the least square method for the best curve-fitting materials corresponding to the Mooney-Rivlin, Ogden, and Neo Hookean models. The results show a perfect agreement with Ogden hyperelastic model compared to the experimental studies. Moreover, based on our results, we have developed the three-dimensional finite element (FE) models by simulation of esophageal dynamic movements. Hence, FE analyses are taken into account for both simplicity and simulation of esophageal peristaltic behavior. By the numerical solutions, an interactive coding between MATLAB and ABAQUS software have been developed to achieve our goal. Current investigation is an effort to simulate esophagus, which would be used as a predictable tool for the medical and physio-mechanical study as well as educational purposes.

Keyword: tissue mechanics; hyperelastic theory; esophageal behavior; physio-mechanics; finite element modeling

Received: 7 June 2019, Accepted: 21 June 2019

DOI: 10.22034/jbr.2019.189018.1009

1. Introduction

One out of 17 individuals would progress some type of dysphagia during their living [1]. Any malfunction in normal physiology of the swallowing process is known as dysphagia [2]. Computational modeling of the esophageal normal physiology is the crucial factor in light of medical diagnosis and advanced research purposes. There are plenty of reasons condensed in the literature for the computational modeling and numerical simulations regarding to human physiology as well as esophageal behavior [3-8].

The esophagus - a hollow cylinder normally 25-30 cm in length with approximately 2.5-3 cm in diagonal [9] - has limited accessibility for its recognition and physiology. Primarily, experimental attempts made numerous progress within esophageal interpretation. Some of them were described more in detailed in a review article by [10]. Some others with an engineering point of view have elucidated by [4, 11-13]. Besides the reliable consequences, those experiments are restricted methods, which drew out particular outcomes. As an example, esophageal monometry, the standard test for the measurement of

esophageal intraluminal pressure, illustrates the pressure of peristaltic behavior and bolus (food) transport during the swallowing process. In addition, the video fluoroscopy, a method to record the video of swallowing procedure using barium swallow, demonstrates the geometrical patterns of esophageal motility along with bolus transport [10, 14]. Although conventional manometry and video fluoroscopy are now shifted to the high resolution manometry and digital video fluoroscopy, the results still portray sole outcomes, which are intraluminal pressure and geometrical variations [15, 16].

Compared to the experimental studies, a computer simulation of an internal organ would depict variety of outcomes as well as a perceptible model [3, 6, 7]. For this purpose, understanding the biomechanical properties of the tissue layers is the prerequisite of basic investigations toward a computational simulation. With regard to the histological study, biological soft tissues (like esophagus) are known as nonlinear, anisotropic and incompressible materials [17, 18]. From the experimental point of view, esophagus tissue is characterized as a two-layer organ, mucosa-submucosa (m-s) and muscle (muscularis) layer [19-24]. In the research by Yang et al., tissue layers of the porcine esophagus were studied under the uniaxial and inflation testing in both axial and circumferential direction [19, 20]. Moreover, concerning the obtained results by Yang et al. a mathematical model was developed for deeper understanding toward the biomechanical behavior of the esophagus tissue [21]. Alternatively, a comprehensive study by Sommer et al. scrutinized tissue mechanics of ovine esophagus in the multiaxial direction [22]. Subsequently, the microcontinuum model adjusts appropriate fit to the function of the layers of porcine esophagi [24]. Furthermore, the results of mechanical testing on human cadaveric esophagus portrayed the stress-strain behavior of the whole tissue, was reported by [23]. In addition, the computational models of gastrointestinal (GI) tract along with esophageal motility were reviewed by [25]. They also explored a two-layer finite element (FE) study of the esophagus model to characterize mechanical behavior of esophageal tissue layers [26]. Simulating esophagus soft tissue layers, part of this study is the comparison between different models through hyperelastic theory in light of achieving a simple and effective model. Comparing three constitutive models by using the least square method, we have characterized the biomechanical behavior of m-s and muscularis layer.

Considering the complexity of esophageal peristaltic behavior and its tissue mechanics, we have created a three-dimensional (3D) FE model, as an applicable tool, to demonstrate various outcomes. In the Yang et al. headway, esophageal bolus transport and its wave-form (peristalsis) movement was simulated using FE method [27]. Moreover, 3D model of the human gastroesophageal (GE) junction and esophagus body by [28, 29], in respect of development of the *Physiome Project*, was used to discriminate between tissue layers and mechanical behavior of GE junction. Afterwards, a manually constructed 3D model of the upper gastrointestinal (GI) tract extracted from *Visible Human Project* database was made to expand useful information for simulation study, physiological and pathological variations [30]. Even though those studies were major efforts on esophageal modeling, certain upshots and specific simulations restricted their work as well. Current modeling could propel future simulation of the esophageal study. It would also be a solution for the purpose of concurrent examination as a time-dependent tool [3, 7].

Therefore, the aim of current study is to obtain an appropriate model from which computational layers could potentially simulate esophageal peristaltic behavior and its tissue mechanics. Hence, the Mooney-Rivlin, Ogden, and Neo Hookean models, based on the hyperelastic theory, were studied compared to experimental results. Additionally, simulating esophageal peristaltic behavior, the active intraluminal pressure of the swallowing transport has been applied to the FE layers. It should be noted that the whole organ (esophagus) is simulated as a 3D cylinder, consisting of m-s and muscularis layer, in its three regions known as: cervical, thoracic, and abdominal.

2. Materials and methods

2.1. Experimental data

The obtained data were extracted from experimental study carried out by [19] to achieve the mechanical behavior of the esophagus tissue layers. In their study, uniaxial tensile test on fresh porcine esophagi was taken into account. The pigs were 3-4 months old and weight 70-80 kg. Tissue layers of the esophagus were segregated into the mucosa-submucosa (m-s) and muscularis layer. All segments were cut from the cervical, thoracic, and abdominal regions into the grip-to-grip dog bone shapes. Each tissue of segments was consisted a value of 25 mm in length and 5 mm in width. It is worth nothing that the mean value of thicknesses was varied between m-s and muscularis layer from 2 mm to 3 mm, respectively. All the samples were tested under the uniaxial tensile tests in both circumferential and axial orientation. In addition, the load-to-failure test was set on the strain rate of 50 mm/min [19]. In both m-s and muscularis layers, the average value of stress-strain function from experimental tests have been used for the curve fitting analysis (section 2.3).

The physiological loadings affecting esophageal motility were acquired from a concurrent manometric and fluoroscopic study performed by [16], Table 1. The study was done on 20 healthy subjects, 7 men and 13 women between 20 to 45 years old. A solid-state high-resolution manometry, divided in 1 cm interval with 36 circumferential sensors, has been used to measure the intraluminal pressure inside of esophageal body. Moreover, the barium swallows- a routine method for the swallowing characterization- were recorded with two 5 ml and one 10 ml barium swallow. Furthermore, the range of 0 to 100 mmHg was calibrated for the preceding records [16].

2.2. Constitutive models

Low elastic and bulk modulus material models with large deformations, which are path-independent, are known as hyperelastic materials. These are described in term of the strain energy potential, which defines the strain energy stored in the material per unit of reference volume (volume of initial configuration) as a function of deformation [17]. Many hyperelastic models have been developed and used for soft tissue materials. In this research, we had a comparison between three widely used models, Mooney-Rivlin, Neo Hookean, and Ogden model [31, 32] to find an appropriate model for the esophagus tissue layers.

2.2.1. Ogden model

The Ogden model is represented for hyperelastic material in the form of strain energy potential as below [33]:

$$U = \sum_{i=1}^{N} \frac{2\mu_i}{\alpha_i}(\bar{\lambda}_1^{\alpha_i} + \bar{\lambda}_2^{\alpha_i} + \bar{\lambda}_3^{\alpha_i} - 3) + \sum_{i=1}^{N} \frac{1}{D_i}(J_{el} - 1)^{2i} \quad (1)$$

here U is the strain energy potential, and $\bar{\lambda}_i$ are the deviatoric principal stretches that can be further expressed as follows:

$$\bar{\lambda}_i = J^{-\frac{1}{3}}\lambda_i \quad (2)$$

In the aforementioned equation, J is the volume ratio and λ_i refers to the principal stretches. In equation 1, material constants are N, μ_i, α_i and D_i in which μ_i and α_i describe the shear behavior of material and D_i indicates the range of compressibility (D_i is equal to zero for incompressible materials). Additionally, the principal stretches are related to the principal nominal strains by:

$$\lambda_i = 1 + \varepsilon_i \quad (2)$$

Moreover, J is the ratio between present volume to the initial volume (the determinant of deformation gradient matrix, F) and is obtained from the below relation:

$$F = \begin{bmatrix} \lambda_1 & 0 & 0 \\ 0 & \lambda_2 & 0 \\ 0 & 0 & \lambda_3 \end{bmatrix}, J = \det(F) = \lambda_1\lambda_2\lambda_3 \quad (3)$$

thus for incompressible materials:

$$\lambda_1\lambda_2\lambda_3 = 1$$

In addition, the elastic volume ratio (J_{el}) is the fraction of (J) -the volume ratio- to the (J_{th})-thermal volume ratio- presented in equation 5:

$$J_{el} = \frac{J}{J_{th}} \qquad (5)$$

Where:

$$J_{th} = (1+\varepsilon^{th})^3 \qquad (6)$$

ε^{th} is the linear thermal expansion strain. Assuming the absence of thermal strain: $J_{th} = 1 \Rightarrow J_{el} = J$ It should be noted that, in equation 1, N could be 1, 2 or 3. By increasing N from 1 to 3, the number of required constants, describing the material behavior, will be increased from 3 to 9. As a result, the cost of calculation, but the precision of curve fitting will be improved significantly. For instance, by choosing $N=2$ and fitting the material parameters, the behavior of curves can be described more accurately; this is discussed more in detailed in section 2.3.

2.2.2. Neo Hookean model

This model is the specific type of Polynomial function from which the general form of Polynomial strain energy potential was represented in equation 7:

$$U = \sum_{i+j=1}^{N} C_{ij}\,(\bar{I}_1-3)^i\,(\bar{I}_2-3)^j + \sum_{i=1}^{N}\frac{1}{D_i}(J_{el}-1)^{2i} \qquad (4)$$

where, N, C_{ij}, and D_i are material constants and $\bar{I}_1$ and $\bar{I}_2$ are the first and second invariants of the deviatoric strain.

$$\bar{I}_1 = \bar{\lambda}_1^2 + \bar{\lambda}_2^2 + \bar{\lambda}_3^2,$$

$$\bar{I}_2 = \bar{\lambda}_1^{(-2)} + \bar{\lambda}_2^{(-2)} + \bar{\lambda}_3^{(-2)} \qquad (8)$$

Particular *form of Polynomial models is obtained by setting the specific coefficients to the zero. If all* C_{ij} *with* $J \neq 0$ *are set to zero, the reduced Polynomial form is achieved. For* $N=1$*, the reduced Polynomial model could be translated to the Neo-Hookean model [34, 35]:*

$$U = C_{1,0}(\bar{I}_1 - 3) + \frac{1}{D_1}(J_{el}-1)^2 \qquad (9)$$

2.2.3. Mooney-Rivlin model

In the general form of Polynomial model, N is set into one, to obtain the Mooney-Rivlin model [36, 37]:

$$U = C_{0,1}(\bar{I}_2 - 3) + C_{1,0}(\bar{I}_1 - 3) + \frac{1}{D_1}(J_{el}-1)^2 \qquad (5)$$

Assuming the incompressibility*, tissue behavior is described by the two parameters of Mooney-Rivlin model,* $C_{0,1}$ *and* $C_{1,0}$*.*

2.3. Curve fitting method and analysis

The least square method- a standard numerical method- is used to fit three hyperelastic constitutive models with experimental outcomes. In this method, complex equations such as nonlinear functions are being fitted based on the minimal sum of the errors or the least deviation squared. Considering a set of experimental stress and strain data as (σ_1, ε_1), (σ_2, ε_2), (σ_3, ε_3), (σ_n, ε_n), the sum of square errors is defined as below:

$$S_{err} = \sum_{i=1}^{n} err_i^2, err_i = \sigma_i - f(\varepsilon_i, p) \qquad (11)$$

Table 1. Physiological loadings in term of intraluminal pressure [KPa] [16]

Time [S] \ Length of Esophagus [Cm]	0	2	4	6	8	10	12	14	16	18	20	22	24	25
0	**4.00**	0.27	0.13	0.00	0.00	0.13	0.40	0.13	0.40	0.40	0.00	0.00	2.00	1.87
2	4.00	**5.00**	**1.67**	0.53	0.53	0.40	0.53	0.53	0.40	0.40	0.40	0.53	1.33	1.33
4	4.00	1.07	**2.67**	**3.73**	**2.27**	1.33	0.67	0.53	0.53	0.67	0.67	0.67	0.67	1.07
6	4.00	0.53	0.53	1.07	**1.33**	**3.73**	**6.67**	**8.00**	**4.93**	1.07	0.67	0.80	0.80	0.80
8	4.00	0.27	0.13	0.00	0.13	0.80	1.67	**4.00**	**5.33**	**10.00**	**8.67**	1.33	1.07	0.80
10	4.00	0.53	0.13	0.00	0.13	0.67	0.80	0.93	2.40	**7.07**	**12.00**	**4.00**	1.67	1.07
12	4.00	0.53	0.27	0.00	0.00	0.00	0.40	0.13	0.67	0.80	**3.73**	**3.73**	**3.33**	2.00
14	4.00	0.27	0.13	0.00	0.00	0.27	0.67	0.13	0.53	0.53	0.13	0.13	**4.00**	**2.67**

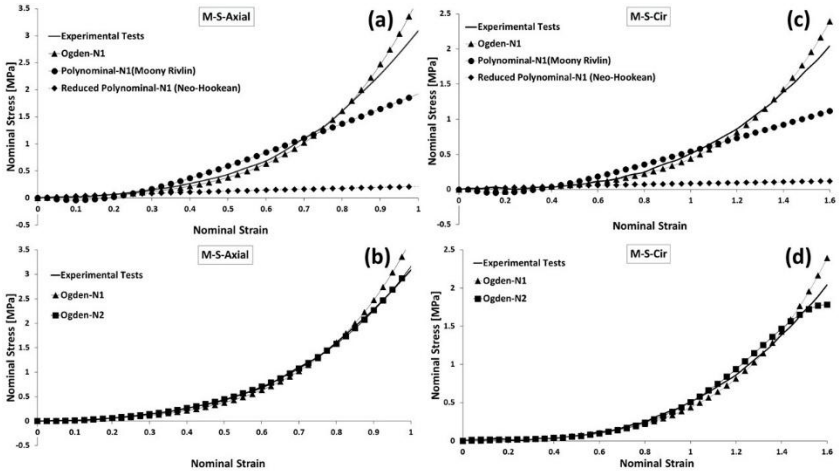

Figure 1. Curve fitting of the *m-s layer* with constitutive models. (a), (b) *axial* (c), (d) *circumferential* direction

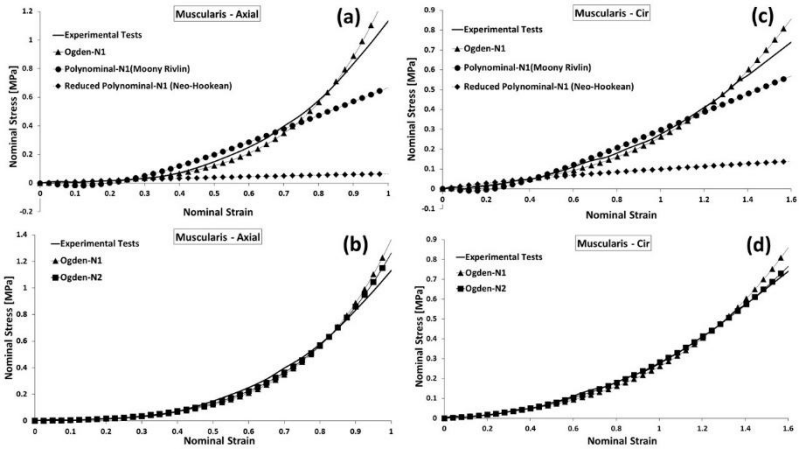

Figure 2. Curve fitting of the muscularis layer with constitutive models. (a), (b) axial (c), (d) circumferential direction

The *f* function is defined hyperelastic behavior of the materials. In addition to the variable strain (ε), this function also depends on the vector parameters (p). The length of p must be less than *n*. The goal is to find p so that S_{err} is minimized. Further information concerning the least square method could be find in [38]. The curve-fitting analyses for constitutive models were done using ABAQUS v6.12. The comparsion between three hyperelastic constitutive models, Moony Rivlin, Neo Hookean, and Ogden, were indicated in Fig. 1 and 2. Both uniaxial and circemferential direction were taken into account for the m-s and muscularis layer. In the figures (1 and 2) the continuous black lines are the results refered to Yang et al. study [19]. While both layers were in perfect match with Ogden hyperelastic model, (Fig. 1 and 2), it was expanded up to the six-parameter (Ogden-N2) to fit the curves more accurately. This is shown on Fig. 1, b and d as well as on Fig. 2, b and d.

2.4. Root mean square

Calculating the errors between FE tissues and in-vitro tests of the esophagus tissue layers, the root mean square error (RMSE) is used to compute the percentage error between two matrices [39]. Based on the sum of the average square errors between the obtained FE and experimental (Exp) strains $(\varepsilon_{1Exp}-\varepsilon_{1FE}),(\varepsilon_{2Exp}-\varepsilon_{2FE}),...,(\varepsilon_{lExp}-\varepsilon_{lFE})$ the RMSE is described as below:

$$RMSE=\sqrt{\sum_{i=1}^{l_{Exp}}(Exp-FE)^2/l_{Exp}}\times 100 \quad (6)$$

where RMSE is the percentage error between the obtained strains from Exp and FE results. The l_{Exp} is the number of data from Exp strains, equal to the FE strains, which is used in equation 12.

2.5. Finite element analysis

As previously mentioned, the finite element (FE) method has been used for the analysis of the models. Domain discretization to the finite element is the initial step in FE method. For this purpose, a mesh generation function is coded in MATLAB. This function discretizes the geometry according to the design variable data from the normal esophagus. The final product is to export a text file as an input-file for the analysis software. The procedure of FE modeling has been shown in the flowchart of Fig. 3.

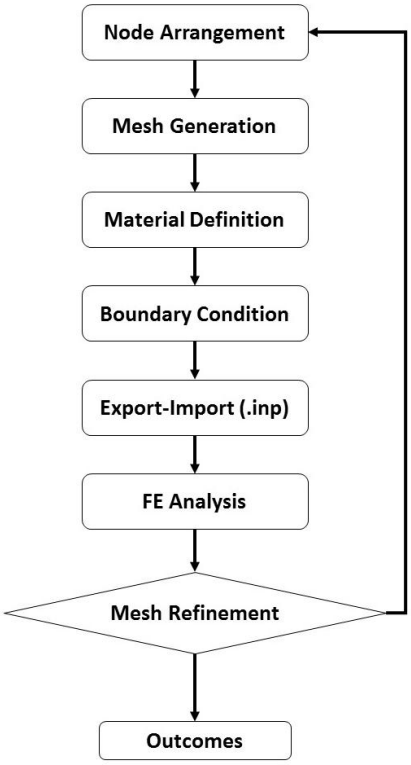

Figure 3. The process of FE modeling

2.5.1. Geometry of the model

To generate the meshes, coordination of the nodes was obtained and then the constituent nodes of each element were assigned to it. For this purpose, the esophagus was divided into the layers with thickness l_z where z coordinate is constant for the nodes in each level. The polar system was utilized to calculate x and y coordinate of the nodes. Esophagus ring is divided with equal angles and the distance of the nodes from the center is calculated (Fig. 4). Then x and y coordinate of each node was received a form of polar to the Cartesian system. Iterative process on

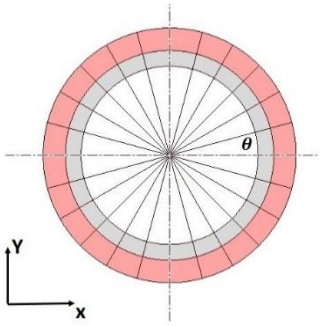

Figure 4. Obtaining the coordinate of the nodes in a slice of esophagus

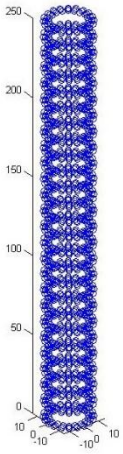

Figure 5. *Nodes in the model of esophagus*

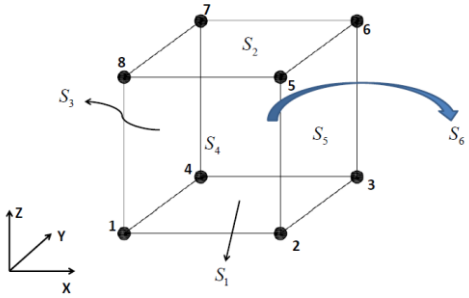

Figure 6. *Eight nodes brick element*

this step, the coordination of the nodes in all levels calculated and finally all nodes of the domain were defined (Fig. 5).

The nodes are numbered from bottom to top, center to outside and in counter-clockwise direction. By obtaining the node numbers, which are connected to each element, esophagus modeling is accomplished. Eight nodes brick element is utilized in FE analysis. The sequence of numbering and the surface definition of this element are shown in Fig. 6.

The elements are numbered in the same way as nodes. Thus, after obtaining the number of nodes in the first element on each level, the number of nodes in other elements are provided by a linear function of the element number. Fig. 7 shows the final model made by mesh generation function. Ultimately, some of the nodes and elements are defined as special sets such as interior, exterior surfaces and set of the elements located at the same level and the end nodes. These sets are used to apply loads, boundary conditions, and interactions in the ABAQUS software.

2.5.2. Finite element models

Simulating esophageal peristaltic motility, three finite element (FE) models have been created to approach our aim. The first two ones were simulated esophagus tissue layers and their characterization, while the second one was mimicked esophageal peristaltic motility. In the Fig. 8, discrete layers are depicted along with two-layer FE model of the esophagus body. The m-s and muscularis layer are shown in gray and red color, respectively.

For FE tissues, the rectangular form has been shaped in 25x5 mm. The thicknesses are 2 mm, 3 mm for m-s and muscularis layer (Fig. 8). Both models have the same size as what has been tested at [19]. Moreover, esophageal modeling, a two-layer cylinder containing m-s and muscularis layer, was developed based on the normal size of esophagus body, length=250 mm, D_{out}=25mm [9] (Fig. 8). From the computed tomography (CT) studies on the wall of esophagus body, the calculated mean thickness is 4.34 mm for females and 5.26 mm for males [40]. In light of FE esophagus thickness, female values have been used due to larger number of the female subjects in [16]. It is remarkable that esophagus body is

Figure 7. *Finite element model of esophagus*

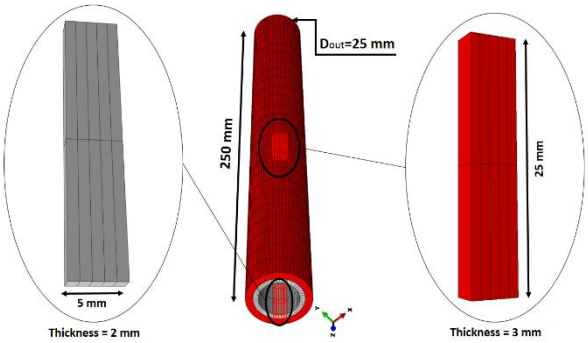

Figure 8. Two layered FE esophagus along with tissue models, m-s (gray) and muscularis layer (red)

divided in three main regions, cervical, thoracic, and abdominal [41].

Hence, for variable thicknesses through the length of FE esophagus, the value of 2.2, 4.1, and 5.3 mm have been applied for the cervical, thoracic, and abdominal regions, respectively [40] (Fig. 9, the right cylinder). With regard to the mean size of muscularis (3 mm) and m-s (2 mm) thickness [19] a ratio of 1.5 (3:2=1.5) was applied to divide the aforementioned thicknesses for the two-layer FE esophagus (m-s and muscularis layers).

2.5.3. Material properties and assumption evidences

We have assumed esophagus tissue layers, nonlinear, incompressible and homogenous isotropic material. The three-parameter form of Ogden hyperelastic model (N1) were taken into account based on the comparison presented in Fig. 1 and 2, section 2.3. In both, FE tissues and FE esophagus, same coefficients obtained from the curve-fitting analysis were set as the material *modules*. The density was calculated about 1050×10^{9}[kg/mm^3] similar to muscular tissues [42]. With regard to histological knowledge, the nonlinear function from axial direction in Fig. 1-a, and circumferential characterization in Fig. 2-a, were considered for the m-s, and muscularis layer, respectively. Furthermore, in the current project the modeling of esophageal sublayers, such as adventitia or longitudinal muscle in the muscularis layer are not taken into account [18, 22, 41].

2.5.4. Preprocessing conditions

In FE tissues, the analysis was set on the static step with eight-node brick elements. Moreover, the acquired results (coefficients) from three-parameter form of Ogden model (N1), depicted in Fig. 1 and 2, were taken into account for FE tissues, section 3.1. It worth nothing that the coefficients from axial direction were set for the FE m-s and circumferential ones in FE muscularis for both models. In the FE esophagus, achieving time dependent analysis, the dynamic-explicit analysis with explicit eight-node brick elements have been set to investigate peristaltic motility as well as tissue deformities. The boundary conditions have been applied on FE models is presented in the schematic view in Fig. 9. From left to right, m-s is stretched in axial and muscularis layer in the circumferential direction. Furthermore, FE esophagus was fixed against all six degree of freedom (DOF) except displacement on z-axis at the end of abdominal region.

2.5.5. Simulation

In FE tissues, both m-s and muscularis layer were analyzed under the same loading condition as Yang et

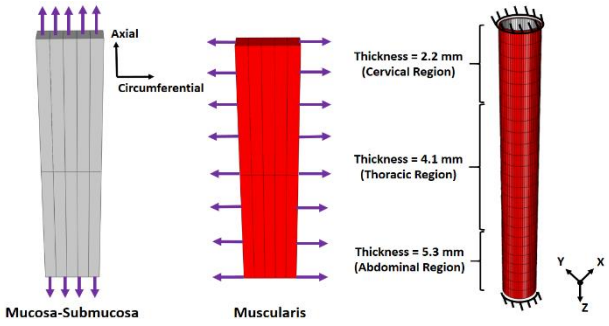

Figure 9. FE models and boundary conditions

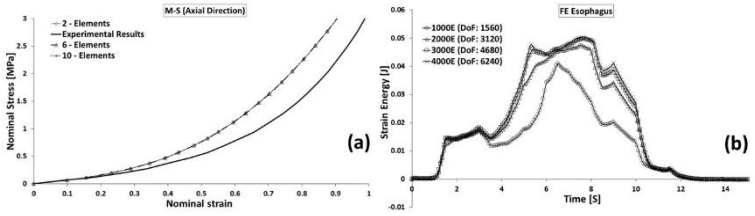

Figure 5. Mesh refinements and convergence solution

al., study [19]. This was shown in Fig. 1 and 2. Furthermore, no boundary conditions have been utilized in the simulation process except the equal pressure in an opposite direction (Fig. 9). Heeding the loading rate: the m-s layer has been stretched in axial direction from 0 to 3.07 MPa and a pressure range of 0 to 0.8 MPa was taken into account for the muscularis layer in circumferential direction (Fig. 9).

Fig. 9 FE models and boundary conditions For FE esophagus, active vivo pressures of the swallowing procedure [16] have been assigned inward of the model to simulate the physio-mechanics of esophageal behavior. The whole body was separated in 25 segments through z-axis (Fig. 9). According to Table 1 each segments took their own loading within an interval of 0.5 second. The sequence leads to a simulation of the muscle contractions and esophageal peristalsis motility.

2.5.6. Mesh refinements and convergence solution

Upon the convergence of the outcomes, in an iterative process, the models have been ran within mesh-size reduction known as h-refinement method [43]. The DOF numbers (node numbers) are increased in both FE tissues and FE esophagus to investigate the stress-strain and strain energy function, respectively (Fig. 10). In the tissue models, the number of elements were increased from two up to ten within a comparison of the strain results in Fig. 10-a. These data were compared to the mean stress-strain curves extracted from experimental tests [19]. The same process has been done for the muscularis layer as well. The goal is to find accuracy of the outcomes with finer mesh numbers. Hence, for FE esophagus, the iterative process in the form of strain energy function has been done until its convergence. Strain energy results demonstrated similar behavior for FE esophagus with 3000 elements and greater (Fig. 10-b). The procedure was carried out using ABAQUS/explicit v6.12 package. The CPU time was about 3 hours for the analysis of FE esophagus (the 3D cylinder).

3. Results

3.1. Outcomes from FE tissues and model validation

From the curve fitting analysis through three constitutive models (Mooney-Rivlin, Ogden, and Neo Hookean), the coefficients of the fitted (Ogden) hyperelastic model is indicated in Table 2. The curves of Ogden model were compared within the original functions obtained from experimental study [19]. Significantly, the root mean square errors (RMSE) (defined in section 2.4) were equal or below 1% for both layers in both directions. Considering equation 1 in section 2.2.1 and the aim of incompressibility in the current study, the invariable D is zero in both three and six parameter form of Ogden model (Table 2).
To double check the accuracy of the obtained coefficeints, the used data from Ogden model (N-1) in Table 2 scrutinized with an analogy between FE tissues and experimental results. Predictably, FE tissues were modeled by Ogden coefficients behaved closely to the mean outcomes from experimental results.

Table 2. The coefficients of the Ogden hyperelastic models, obtained from curve fitting analysis

Model \ Layer	Muscularis		Mucosa-Submucosa	
	Axial	***Circumferential***	***Axial***	***Circumferential***
Ogden N-1	μ = 3.29E-02	μ = 3.42E-02	μ = 0.19	μ = 5.00E-02
	α = 8.12	α = 5.34	α = 6.65	α = 5.85
	D = 0	D = 0	D = 0	D = 0
	(RMSE = 0.6 %)	*(RMSE = 0.9 %)*	*(RMSE = 0.8 %)*	*(RMSE = 1 %)*
Ogden N-2	μ_1 = 1.45E-06	μ_1 = 6.80E-02	μ_1 = 3.88E-02	μ_1 = 4.80E-05
	α_1 = 21.42	α_1 = 5.09	α_1 = 8.97	α_1 = 13.46
	D_1 = 0	D_1 = 0	D_1 = 0	D_1 = 0
	μ_2 = 5.99E-02	μ_2 = -5.10E-02	μ_2 = 0.18	μ_2 = 5.69E-02
	α_2 = -16.39	α_2 = -10.53	α_2 = 4.57	α_2 = 5.24
	D_2 = 0	D_2 = 0	D_2 = 0	D_2 = 0
	(RMSE = 0.6 %)	*(RMSE = 0.9 %)*	*(RMSE = 0.8 %)*	*(RMSE = 1 %)*

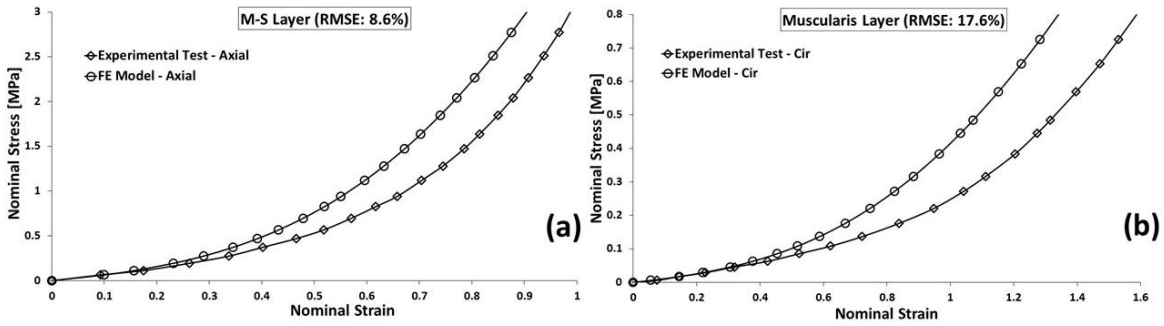

Figure 11.The comparison of FE tissues with experimental tests [19]. (a) m-s layer in axial direction (b) muscularis layer in circemferetial direction.

The above diagrams in Fig. 11 indicate FE tissues stretched in the uniaxial direction. The analysis of both layers (in Fig. 9), were compared to the outcomes from similar conditions in the m-s and muscularis samples of [19] report.

3.2. Outcomes from FE esophagus and verification study

Concurrent coding and simulation leaded FE esophagus to be a computational model of esophageal motility. The written code is a potential tool to apply variety of conditions. The simulation of peristaltic motility was the prime outcome from FE esophagus. In Fig. 12, tissue motility of the layers along the length of FE esophagus is indicated sequentially. Simulating esophageal peristaltic behavior, the time dependent wave-form movements have been mimicked the swallowing procedure.

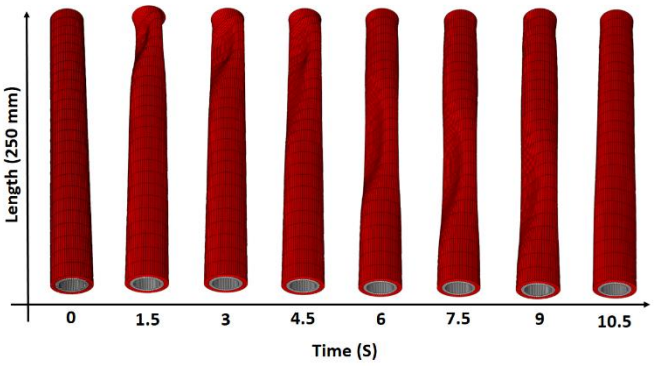

Figure 12. FE esophagus, simulation of esophageal peristaltic motility

3.2.1. Accuracy in geometry (anatomical model)

Seeking model accuracy, geometrical information from esophagus image had been used to achieve a more precise FE esophagus (Fig. 13). Information of esophageal border borrowed from free access image on digital lab 3D website (www.turbosquid.com), except the data size relevant to the esophageal geometry, same process (described in section 2.5) had been utilized toward the peristaltic simulation of anatomical model.

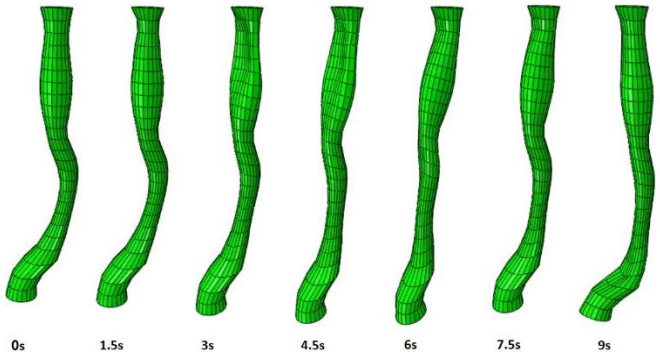

Figure. 6 Simulation of peristaltic behavior in real geometry

3.2.2. Layer displacement in FE esophagus with accurate geometry

Layer characterization and time dependent prediction is a prerequisite for esophageal peristaltic behavior. Considering esophagus as a luminal organ, the results had been extracted from the polar coordinate system, which was set in ABAQUS visualization module. In Fig. 14, U1 is representing displacement variation through FE esophagus. Based on the legends in Fig. 14, from blue to red, displacement value is going to be greater.

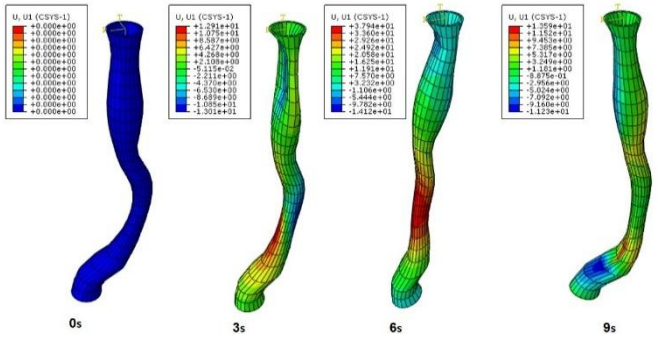

Figure 7. Layer diversity through FE esophagus with accurate geometry

3.2.3. Mesh refinement

Fig. 15 is representing mesh refinement for the anatomical geometry of FE esophagus in Fig. 13. Its procedure was as similar as what had been described in section **Error! Reference source not found.**. The convergence solution was defined by decreasing the element numbers from 3000 to 500. This was occurred due to the refinement of FE esophagus with 3000 elements in section **Error! Reference source not found.**, Fig. 10-b. This was an analogy through strain energy function of FE esophagus in ABAQUS, visualization module. Even though mesh size reduction makes less RMSE, the results in Fig. 15 shows a rational answer for the anatomical model with 1000 elements.

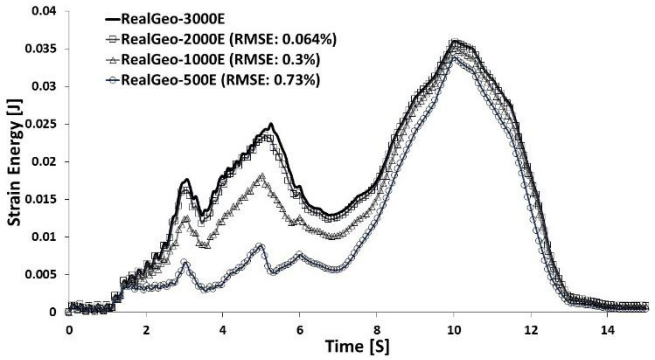

Figure 8. Mesh refinement and convergence solution for FE esophagus in real geometry (anatomical model)

3.2.4. Material investigation and validation study

To investigate the effect of material properties on FE esophagus, a sensitivity analysis had been done applying different materials. The Ogden hyperelastic model was compared with Neo Hookean hyperelastic and rubber-like material (Fig. 16). Surprisingly, the strain energy outcomes were too different in FE esophagus defined with latter materials in comparison with material properties on **Error! Reference source not found.**. It should be noted that the rubber-like material was analyzed based on the elastic theory, where the Poisson's ratio and Young's modulus were 0.4999 [44] and 10 MPa [45], respectively. Moreover, hyperelastic functions from curve fitting analysis (section 2.3) had been considered as well. However, the Moony Rivilin hyperelastic model was not converged with the simulated FE esophagus. Interestingly, the extracted results from visualization module in ABAQUS portrayed diverse characterization in comparison with FE esophagus based on the Ogden model. Large values of the RMSE in Fig. 16 are representing model dependency on the material functions.

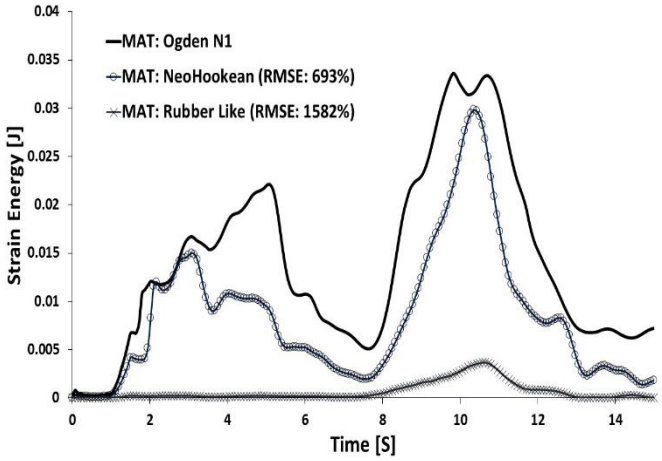

Figure 9. Material investigation, validation study

3.2.5. Bolus clearance, swallowing procedure

Esophagus, as a luminal organ is a link between mouth to stomach with the mission of bolus transport [10]. Final application of FE esophagus was to test bolus clearance and simulation of the swallowing process without gravity intervention. To achieve this goal, a bolus prticle in spherical shape (D=8 mm) had been located into the transition zone [15] of the real FE esophagus (Fig. 14). Solid bolus particle, defined similar to the rubber-like material (section 3.2.4), with frictionless interaction between FE esophagus and bolus particle. The final product was simulation

of the swallowing process along with bolus transport. The full video of bolus transport in Fig. 17 is enclosed to this paper as well.

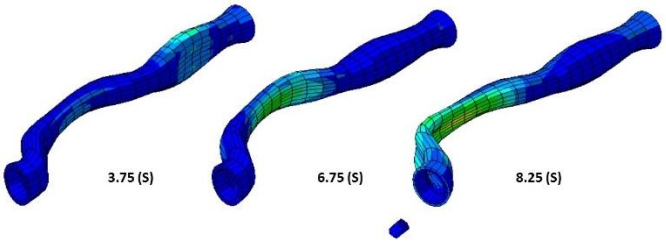

Figure 17. Bolus transport

4. Discussion

In the current study, step-by-step investigation of esophageal simulation was carried out using tissue study and concurrent numerical-biomechanical modeling. Simulating mechanical characterization of the esophagus tissue layers, three constitutive models (Mooney-Rivlin, Ogden, and Neo Hookean) based on the hyperelastic theory were explored by applying curve-fitting analysis. Considering the results from the least square method on Table 2 and outcomes from curve-fitting study (section 2.3); both, three and six parameter form of Ogden hyperelastic models (N1 and N2) were appropriated for the esophagus tissue modeling. The three-parameter model has been used to simulate esophagus tissue layers. We have found that, this is an approved modeling by the calculation of the RMSE in Table 2, where the errors are less than 1%. Moreover, FE tissues were compared to the experimental study by applying similar process, which was done in Yang at el. report [19]. Even though, the comparison was between FE isotropic models and anisotropic in-vitro tissues, the RMSE for m-s layer is below 10% (Fig. 11-a), while it is 17.6% for the muscularis layer (Fig. 11-b). There are crucial reasons for making FE tissues as the verified models with acceptable errors. First, the used experimental results are average functions from in-vitro tests on the pig samples. Second, tissue samples are extracted from different parts of the esophagus, known as cervical, thoracic, and abdominal segment (section 2.1) [19]. Third, both m-s and muscularis layers have their own affect in the opposite direction. As an example, according to the esophagus histology, the muscularis layer is consist of the longitudinal and circular muscles. Normally, these are reinforced by the natural muscle fibers in their own direction [6, 7, 18, 21, 22]. Hence, not all details have been simulated in our FE tissues. However, the question is, do we need all details to have a practical esophagus? To answer this question, we suggest future studies to investigate the effect of esophageal sublayers in the computational format regarding to peristalsis motility.

Obviously, there are distinct differences between current FE esophagus and other models in literature. In the [27] study, the axisymmetric FE analysis was used for the prediction of particular diseases in esophageal malfunction and mechanical characterization. Moreover, [28] have simulated GE junction to predict biomechanical behavior of its tissue layers. Subsequently, 3D model of the upper GI tract by [30] provided applicable facts for the future simulation of physiological and pathological study.

In our MATLAB-ABAQUS code, esophageal peristaltic behavior was developed using numerical modeling. This is a potential tool for the current and future physiological study, educational use, and clinical purposes. A consistent coding toward the esophagus simulation, as an intraluminal organ, is a significant achievement. First of all, the applied physiological loadings from barium swallow [16] make FE esophagus to be a time dependent tool for understanding the physio-mechanical behavior of the esophageal motility (Fig. 12 and 14). In addition, sufficient alternative to rework the geometry, regional parts, material properties (Fig. 13 to 16) and or other conditions such as normal and pathophysiological behavior of esophageal motility in FE esophagus. This is a remarkable progress in reference to the recent studies [6, 7, 30]. Indeed, simulation of the swallowing procedure within bolus transport is a novel outcome and a potential application of our work (Fig. 17). Considering duration of the normal bolus transport from upper through lower esophageal sphincter, which is about 8 seconds. As a diagnostic symptom, swallowing transport beyond that limit occurs with esophageal abnormality [6, 46]. Since bolus clearance in Fig. 17 (attached video) is

happened at the aforementioned point of time (≈ 8th second), the model is working properly, in comparison to the normal physiology of bolus transport.

Although, this research is an effort in light of achieving a complete simulation of esophageal peristaltic behavior, there are certain limitations in our work as well. For FE tissues, due to run time reduction, not all details had been applied. Correspondingly, assuming isotropic, homogenous material may affect an exact simulation. Moreover, we have avoided applying the effect of viscoelasticity of the biological soft tissue organs [47-48]. Additionally, more analysis with different boluses need to be considered for the swallowing simulation toward a more precise modeling. Hence, the written code must be developed for an accurate simulation of the whole organ along with bolus particles.

As a systematic method, our FE modeling would be used in the normal and or abnormal study regarding esophageal motility. Even though more study needs to fill the gaps of our work and this area as well, our endeavor is a novel method in prediction of esophageal peristaltic behavior. It is also a potential tool to simulate other luminal-shape organs.

In conclusion, our research presented curve-fitting analysis through three hyperelastic models, which portrayed a good agreement of the Ogden model with esophagus soft tissue layers. Development of a MATLAB code leaded us to generate FE esophagus as a potential tool to understand the physio-mechanical behavior of esophageal peristaltic motility. Using ABAQUS software, we have investigated geometrical and conditional variations in FE esophagus. Moreover, swallowing process along with bolus clearance has been studied using our MATLAB-ABAQUS code. This study is a predictive tool for the future use in medical investigation and clinical therapy.

Acknowledgment

We Thank Mr. Emad Ghahramanian and Lirok Company for their support on this research. We would also like to thank Ms. Fateme Nejatbakhsh for her helpful revision on this paper.

Conflict of interest

The authors declare that they have no conflict of interest.

References

[1] Malagelada J, Bazzoli F, Boeckxstaens G, De Looze D, Fried M, Kahrilas P. World Gastroenterology Organisation Global Guidelines. Dysphagia [Internet]. Milwaukee, WI: World Gastroenterology Organisation; 2014 [accessed 2015 Dec 8]. 2014.

[2] Cook IJ. Diagnostic evaluation of dysphagia. Nature Clinical Practice Gastroenterology & Hepatology. 2008;5:393-403.

[3] Hunter P, Nielsen P. A strategy for integrative computational physiology. Physiology. 2005;20:316-25.

[4] Li M, Brasseur JG, Dodds WJ. Analyses of normal and abnormal esophageal transport using computer simulations. American Journal of Physiology-Gastrointestinal and Liver Physiology. 1994;266:G525-G43.

[5] Gregersen H, Kassab G. Biomechanics of the gastrointestinal tract. Neurogastroenterology & Motility. 1996;8:277-97.

[6] Du P, Yassi R, Gregersen H, Windsor JA, Hunter PJ. The virtual esophagus: investigating esophageal functions in silico. Annals of the New York Academy of Sciences. 2016;1380:19-26.

[7] Gregersen H, Liao D, Brasseur JG. The Esophagiome: concept, status, and future perspectives. Annals of the New York Academy of Sciences. 2016;1380:6-18.

[8] Gregersen H. Biomechanics of the gastrointestinal tract: new perspectives in motility research and diagnostics: Springer Science & Business Media; 2003.

[9] Saladin KS. Anatomy & physiology: WCB/McGraw-Hill; 1998.

[10] Paterson WG. Esophageal peristalsis. GI Motility online. doi:10.1038/gimo13. 2006.

[11] Nguyen H, Silny J, Albers D, Roeb E, Gartung C, Rau G, et al. Dynamics of esophageal bolus transport in healthy subjects studied using multiple intraluminal impedancometry. American Journal of Physiology-Gastrointestinal and Liver Physiology. 1997;273:G958-G64.

[12] Ghosh S, Janiak P, Fox M, Schwizer W, Hebbard G, Brasseur J. Physiology of the oesophageal transition zone in the presence of chronic bolus retention: studies using concurrent

high resolution manometry and digital fluoroscopy. Neurogastroenterology & Motility. 2008;20:750-9.

[13] Dai Q, Liu J-B, Brasseur JG, Thangada VK, Thomas B, Parkman H, et al. Volume (3-dimensional) space-time reconstruction of esophageal peristaltic contraction by using simultaneous US and manometry. Gastrointestinal endoscopy. 2003;58:913-9.

[14] Ren J, Massey BT, Dodds WJ, Kern MK, Brasseur JG, Shaker R, et al. Determinants of intrabolus pressure during esophageal peristaltic bolus transport. American Journal of Physiology-Gastrointestinal and Liver Physiology. 1993;264:G407-G13.

[15] Ghosh SK, Janiak P, Schwizer W, Hebbard GS, Brasseur JG. Physiology of the esophageal pressure transition zone: separate contraction waves above and below. American Journal of Physiology-Gastrointestinal and Liver Physiology. 2006;290:G568-G76.

[16] Ghosh SK, Kahrilas PJ, Lodhia N, Pandolfino JE. Utilizing intraluminal pressure differences to predict esophageal bolus flow dynamics. American Journal of Physiology-Gastrointestinal and Liver Physiology. 2007;293:G1023-G8.

[17] Ogden RW. Nonlinear elasticity, anisotropy, material stability and residual stresses in soft tissue. Biomechanics of soft tissue in cardiovascular systems: Springer; 2003. p. 65-108.

[18] Stavropoulou EA, Dafalias YF, Sokolis DP. Biomechanical and histological characteristics of passive esophagus: experimental investigation and comparative constitutive modeling. Journal of biomechanics. 2009;42:2654-63.

[19] Yang W, Fung T, Chian K, Chong C. Directional, regional, and layer variations of mechanical properties of esophageal tissue and its interpretation using a structure-based constitutive model. Journal of biomechanical engineering. 2006;128:409-18.

[20] Yang W, Fung T, Chian K, Chong C. 3D mechanical properties of the layered esophagus: experiment and constitutive model. Journal of biomechanical engineering. 2006;128:899-908.

[21] Natali AN, Carniel EL, Gregersen H. Biomechanical behaviour of oesophageal tissues: material and structural configuration, experimental data and constitutive analysis. Medical engineering & physics. 2009;31:1056-62.

[22] Sommer G, Schriefl A, Zeindlinger G, Katzensteiner A, Ainödhofer H, Saxena A, et al. Multiaxial mechanical response and constitutive modeling of esophageal tissues: impact on esophageal tissue engineering. Acta biomaterialia. 2013;9:9379-91.

[23] Egorov VI, Schastlivtsev IV, Prut EV, Baranov AO, Turusov RA. Mechanical properties of the human gastrointestinal tract. Journal of biomechanics. 2002;35:1417-25.

[24] Sanchez-Molina D, Velazquez-Ameijide J, Arregui-Dalmases C, Rodríguez D, Quintana V, Shafieian M, et al. A microcontinuum model for mechanical properties of esophageal tissue: experimental methodology and constitutive analysis. Annals of biomedical engineering. 2014;42:62-72.

[25] Liao D, Lelic D, Gao F, Drewes AM, Gregersen H. Biomechanical functional and sensory modelling of the gastrointestinal tract. Philosophical Transactions of the Royal Society A: Mathematical, Physical and Engineering Sciences. 2008;366:3281-99.

[26] Liao D, Zhao J, Fan Y, Gregersen H. Two-layered quasi-3D finite element model of the oesophagus. Medical engineering & physics. 2004;26:535-43.

[27] Yang W, Fung TC, Chian KS, Chong CK. Finite element simulation of food transport through the esophageal body. World journal of gastroenterology. 2007;13:1352-9.

[28] Yassi R, Cheng L, Rajagopal V, Nash M, Windsor J, Pullan A. Modeling of the mechanical function of the human gastroesophageal junction using an anatomically realistic three-dimensional model. Journal of biomechanics. 2009;42:1604-9.

[29] Yassi R, Cheng L, Al-Ali S, Smith N, Pullan A, Windsor J. An anatomically based mathematical model of the gastroesophageal junction. Engineering in Medicine and Biology Society, 2004 IEMBS'04 26th Annual International Conference of the IEEE: IEEE; 2004. p. 635-8.

[30] Gastelum A, Mata L, Brito-de-la-Fuente E, Delmas P, Vicente W, Salinas-Vázquez M, et al. Building a three-dimensional model of the upper gastrointestinal tract for computer simulations of swallowing. Medical & biological engineering & computing. 2016;54:525-34.

[31] Sarma P, Pidaparti R, Moulik P, Meiss R. Non- linear material models for tracheal smooth muscle tissue. Bio-medical materials and engineering. 2003;13:235-45.

[32] Trabelsi O, del Palomar AP, Tobar AM, López-Villalobos J, Ginel A, Doblaré M. FE simulation of human trachea swallowing movement before and after the implantation of an endoprothesis. Applied Mathematical Modelling. 2011;35:4902-12.

[33] Ogden RW. Non-linear elastic deformations: Courier Corporation; 1997.

[34] Macosko C. Rheology: Principles, measurements, and applications. 1994. VCH, New York.

[35] Campion R, Gent AN. Engineering with rubber: Hanser; 2001.

[36] Rivlin R. Large elastic deformations of isotropic materials. IV. Further developments of the general theory. Philosophical Transactions of the Royal Society of London Series A, Mathematical and Physical Sciences. 1948;241:379-97.

[37] Mooney M. A theory of large elastic deformation. Journal of applied physics. 1940;11:582-92.

[38] Kelley CT. Iterative methods for optimization: Siam; 1999.

[39] Kenney J, Keeping E. Moving averages. Kenney JF Mathematics of statics Princeton NJ: Van Nostrand. 1962:59-60.

[40] Xia F, Mao J, Ding J, Yang H. Observation of normal appearance and wall thickness of esophagus on CT images. European journal of radiology. 2009;72:406-11.

[41] Kuo B, Urma D. Esophagus-anatomy and development. GI Motility online. 2006.

[42] Urbanchek MG, Picken EB, Kalliainen LK, Kuzon WM. Specific force deficit in skeletal muscles of old rats is partially explained by the existence of denervated muscle fibers. The Journals of Gerontology Series A: Biological Sciences and Medical Sciences. 2001;56:B191-B7.

[43] Babuška I, Guo B. The h, p and h-p version of the finite element method; basis theory and applications. Advances in Engineering Software. 1992;15:159-74.

[44] Mott P, Roland C. Limits to Poisson's ratio in isotropic materials. Physical review B. 2009;80:132104.

[45] South JT. Mechanical properties and durability of natural rubber compounds and composites. 2001.

[46] Paterson W, Goyal R, Habib F. Esophageal motility disorders. GI Motility Online. doi:10.1038/gimo20. 2006.

[47] Pioletti DP, Rakotomanana LR. Non-linear viscoelastic laws for soft biological tissues. European Journal of Mechanics a-Solids. 2000;19:749-59.

[48] Ahani E, Montazer M, Toliyat T, Mahmoudi Rad M. A novel biocompatible antibacterial product: Nanoliposomes loaded with poly(hexamethylene biguanide chloride). Journal of Bioactive and Compatible Polymers. 2017;32(3):242-262.